

# COMPARISON OF SINGLE TRIAL BACK-PROJECTED INDEPENDENT COMPONENTS WITH THE AVERAGED WAVEFORM FOR THE EXTRACTION OF BIOMARKERS OF AUDITORY P300 EPs

B.W. Jervis<sup>1\*</sup>, S.Y. Belal<sup>2</sup>, K. Camilleri<sup>3</sup>, T. Cassar<sup>3</sup>, S. Fabri<sup>3</sup>, D.E.J. Linden<sup>4</sup>, K. Michalopoulos<sup>5</sup>, M. Zervakis<sup>5</sup>, C. Bigan<sup>6</sup> and M. Besleaga<sup>7</sup>

<sup>1</sup> SoCCE, University of Plymouth, Plymouth, PL4 8AA, England <sup>2</sup> Faculty of ACES, Sheffield Hallam University, Sheffield S1 1WB, England <sup>3</sup> iBERG, Faculty of Engineering, University of Malta, Malta <sup>4</sup> School of Psychology, University of Wales Bangor, Bangor LL57 2AS, Wales <sup>5</sup> Technical University of Crete, Department of Electronics and Computer Engineering, Chania, Greece <sup>6</sup> Ecological University of Bucharest, Bucharest, Romania <sup>7</sup> Romanian Society for Clinical Neurophysiology  
\* Email: keckule@yahoo.co.uk Fax: 00 44 114 225 3433

**Keywords:** Evoked Potential, Independent Component Analysis, P300, biomarkers.

magnitude, ongoing, background electroencephalogram (EEG).

## Abstract

The independent components analysis (ICA) of the auditory P300 evoked responses in the EEG of normal subjects is described. The purpose was to identify any features which might provide the basis for biomarkers for diseases, such as Alzheimer's disease. Single trial P300s were analysed by ICA, the activations were back-projected to scalp electrodes, many artefactual components were removed automatically, and the back-projected independent components (BICs) were first clustered according to their amplitudes and latencies. Then these primary clusters were secondarily clustered according to the columns of their mixing matrices, which clusters together those BICs with the same scalp topographies and, therefore, source locations. The BICs comprising the P300s had simple shapes, approximating half-sinusoids. Trial-to-trial variations in the BICs were found, which explain why different averages have been reported. Both positive- and also negative-going BICs were identified, some associated with known peaks in the P300 waveform. Artefact-free, single trial P300 waveforms could be constructed from the BICs, but these are probably of less interest than the BICs themselves. The findings demonstrate that neither averaged P300s, nor single trial P300s, are reliable as biomarkers, but rather it will be necessary to investigate the BICs present in a number of single trial realizations.

## 1 Introduction

Evoked Potentials (EPs) elicited in a variety of sensory and cognitive paradigms have been commonly used to study brain functions in psychological and clinical research [14] and in the diagnosis of neurological and psychiatric disorders, such as AD and schizophrenia. However, in the analysis of EPs the fundamental problem is to extract information about the potential from measurements that also contain the larger

To increase the signal-to-noise ratio (SNR) conventional analysis of EPs is based on synchronised averaging of realizations, time-locked to the applied stimulus or measured response, assuming trial-to-trial invariability. Nonetheless, responses, reflecting complex brain processes, are likely to present considerable variability due to various factors such as experimental manipulations, level of attention, and quality of performance [2]. This conventional approach has a major drawback as the EPs are time-varying signals reflecting the sum of underlying neural events during stimulus processing. Various procedures such as PCA and repeated-measures analysis of variance (ANOVA) [9] have been employed to separate functionally meaningful events that partly or completely overlap in time. However, the reliable identification of these components in the EP waveform still remains a problem. Independent Components Analysis (ICA) [1] now offers the possibility of extracting the temporally independent components (ICs) of EPs on a single trial basis. The basic P300 waveform is elicited by the oddball paradigm [10], in response to rare "target" stimuli, which are randomly embedded in a sequence of standard stimuli. A number of negative (N) and positive (P) peaks can be observed in the averaged P300 EP waveform, designated N1, N2, P1, P2, and P3, where the numbers indicate the temporal order in which the peaks occur. The occurrence of these different peaks suggests the P300 waveform comprises a number of components. The name P300, used here to describe the response waveform, refers to an important positive voltage maximum, known as the P300b or P3b peak, which occurs from about 300 ms post response to the oddball stimulus. The only consistently occurring peak found in averaged P300s is the P3b and most clinical work has been based upon it.

Various attempts have been made to analyse EPs based on ICA. The EPs were averaged prior to the application of ICA in [4, 6, 15]. However, having used the averaged EPs, any

trial-to-trial variability was ignored and important information might have been lost.

EPs were concatenated in [3, 11, 12] before applying ICA. This is not a truly single trial analysis method. It assumes an unchanged mixing process across all trials. However, if the mixing matrix varies between trials, for physical or computational reasons, concatenation leads to incorrect conclusions, and we have found this to be the case, although we do not report any details here.

A successful application of ICA on EPs was presented in [13] where single trials of visual EPs were analysed and clustered. Only the averaged ICs were shown, and only a small number (256) of samples were used for the analysis, which could have resulted in algorithmic artifacts. In general, our approach appears to be similar to the analysis of VEPs in [13], but the details of our clustering method are different. Furthermore, we have justified our method by comparing our findings with the earlier literature and by testing it by simulations reported elsewhere.

It was decided to investigate the properties of the ICs comprising the P300 of normal, healthy subjects, in order to characterize them and to understand variations in the measured average of the P300 and probable trial-to-trial variations, with a view to the future development of biomarkers for brain diseases and conditions, such as Alzheimer’s disease. To avoid the loss of information associated with averaging and to take into account trial-to-trial variations, the ICA technique was adapted to single trial analysis. Because the ICs are of undetermined magnitude and polarity, their effects at the measurement electrodes (their back-projections) were studied. It was also hypothesized that some of these back-projected ICs (BICs) might be associated with the designated peaks in the P300 waveform.

## 2 Data and methods

### 2.1 Measurements and data

P300 recordings were performed on 9 healthy participants (3 females and 6 males), who had no history of neurological or psychiatric disorder. They were between 37 and 74 years old. P300s were recorded from 27 channels. Linked ears (A1-A2) were used as the recording reference and electrode AFZ was the Ground. Following the standards in [8] signals were digitally sampled at 1024Hz, with a high pass filter of cut-off frequency 0.016Hz, a low pass filter of cut-off frequency 60Hz, and a notch filter at 50 Hz (to remove electrical mains contamination). A stimulator provided 40 2 kHz target tones (20%) and 160 1 kHz non-target tones (80%). The ISI was 1.29s. Subjects were seated with closed eyes, were relaxed, and were instructed to listen carefully and press a button immediately they heard the target tone. A 10s epoch of EEG was recorded for each subject, both before and after the total of 200 tones from the stimulator. 360 target trials were recorded from the subjects (40 per subject). For each of the

target P300s, 599 samples before the stimulus and 700 samples after the stimulus (1300 samples) were taken to form a target single trial P300 lasting 1269.5 ms.

### 2.2 The variability of the averaged P300

Assuming a total number of trials  $n$  collected from all subjects, in order to demonstrate the variability of averaged P300s,  $k$  random subsets, consisting of  $m$  trials selected out of  $n$ , were formed and their averages at electrode Cz were calculated. Then, the P300 peaks were observed on these averaged subsets.

### 2.3 Analysis procedure

The procedure consisted of the application of ICA, artefact removal, feature selection and clustering (Fig. 1), and the study of the peaks of the averaged EP.

#### ICA Procedure

Infomax [1] was applied to the multi-channel EEG of each of the 360 single trials. As a pre-processing step, the raw EEG was whitened by Principal Component Analysis (PCA), included within the Infomax algorithm as a standard procedure.

The resulting activations were back-projected on to electrode Cz, which was identified as the electrode on which the P300 is largest. The BICs which had maxima variance within the interval  $[t_1 t_2] = [586 1036]$  were selected, where the onset of the stimulus occurs at  $t_1 = 586$  ms. and  $[t_1 t_2]$  was chosen to be 450 ms. This is justified by the fact that only the components which appear within  $[t_1 t_2]$  are likely to be related to the EP.

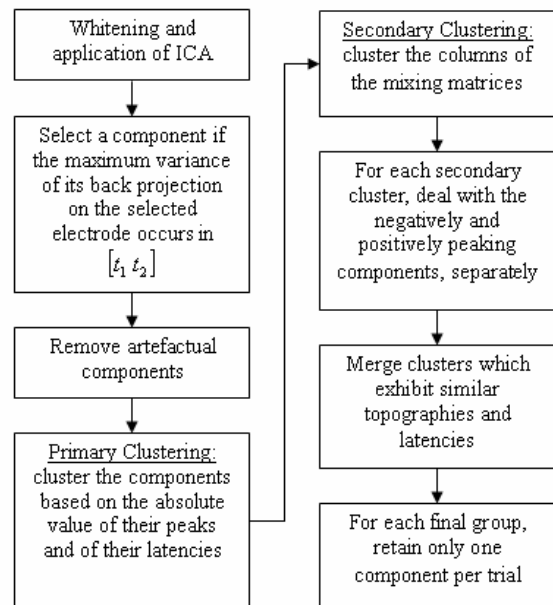
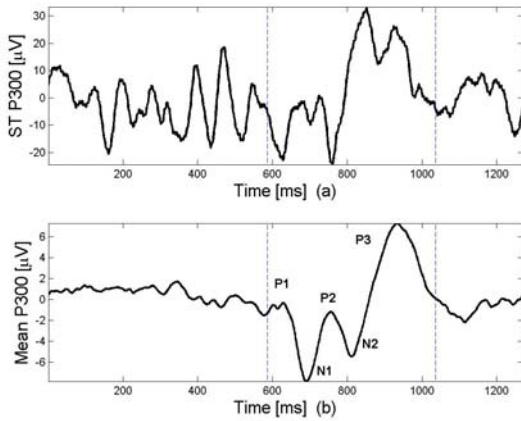


Fig. 1 The steps for extracting the BICs.



**Fig. 2** (a) A single trial P300, (b) the average of 360 trials of the P300 at Cz. Note that the first and last vertical lines mark the interval  $[t_1 t_2]$  in all figures.

### Artefact Removal, Feature Selection and Clustering

Two methods were used for rejecting the noise components. First, if the number of zero crossings of a component after removing its mean exceeded a threshold then it was rejected. Noise-like EEG signals are associated with a relatively high number of zero crossings, while the sparse IC waveforms showed relatively fewer crossings. Similarly, some artefacts are associated with relatively large magnitude peaks compared with the magnitude of the ICs and a similar thresholding procedure was established empirically. Thus, the absolute values of the maxima and minima were calculated for all the independent components, and peaks having amplitudes greater than a threshold were rejected. In both methods the threshold was the sum of the mean and twice the standard deviation of the parameter concerned for all components. These two methods exclude the main artefactual components. Clustering the components in a later stage ultimately separates any remaining artefactual components. From the remaining components, the following features were extracted: the absolute values of the peaks of the back projected components within  $[t_1 t_2]$ , and the latencies of the peaks. These were clustered to satisfy the criterion that each cluster should have similar peaks and latencies.

The unsupervised k-means clustering algorithm [7] was used to group together BICs with similar features. In the adopted procedure, the algorithm was run with different values of  $k$  and the Davies-Bouldin (DB) index [5] was calculated for each run. The  $k$  value which corresponded to the smallest value of the DB index was chosen, and the corresponding clusters were considered to be the correct solution. The resulting clusters contained both negatively and positively peaking components, as expected, since the absolute values of the components' peaks were used as features in clustering. The clusters obtained above were further clustered based on the normalized columns of the mixing matrix corresponding to each component in order to group the components which have similar topographies. This stage of clustering was also

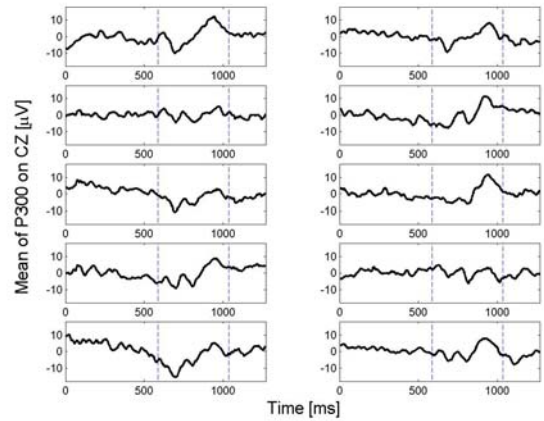


**Fig. 3** The averages of sets of 40 P300 trials selected randomly at Cz.

desirable to group any remaining artefacts found among the independent components.

### The study of the Peaks of the Averaged EP

In order to identify the time intervals within which BICs associated with the peaks in the P300 fall, the following procedure was adopted. The grand average of all P300 recordings for all subjects was calculated, and the latencies of the N1, P2, N2, and P3 peaks within  $[t_1 t_2]$  were identified. The time interval between adjacent peaks were calculated and the smallest chosen. This interval defined the width of a bin centred on each peak, within which associated BICs were considered to fall. All BICs resulting from the application of ICA were used after removing any artefacts. For all trials, the magnitudes of the positive BICs in each bin were recorded, as were the magnitudes of the negative BICs. For each bin, the sum of the positive magnitudes, the sum of the negative magnitudes, and the difference of these sums,  $\Delta M$  were calculated. Also, the single trial P300s corresponding to the positive BICs were averaged, and likewise for the negative BICs. The above procedure was also performed on data from individual subjects. In the following our general findings are illustrated by the results obtained at different electrodes and latencies.

## 3 Results

### 3.1 The variability of the averaged P300

A single trial P300 at electrode Cz and the average of 360 trials recorded from the 9 healthy subjects are shown in Fig. (2a) and Fig. (2b), respectively.

The aforementioned P1, P2, N1, N2 and P3 peaks can be noticed distinctly in Fig. (2b). However, in Fig. (2a) these peaks are less obvious and can be confused with background EEG. This is why averaging is used conventionally for increasing the SNR.

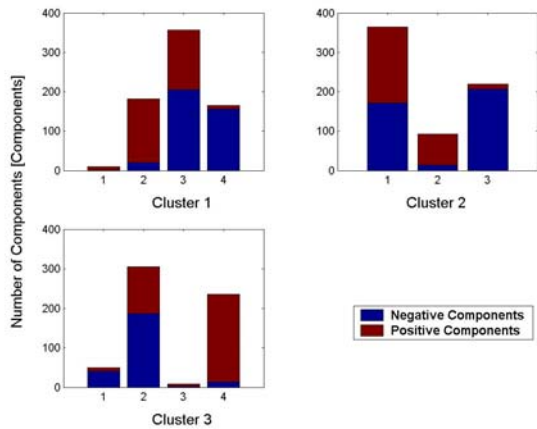


**Fig. 4** The IC groups obtained after clustering.

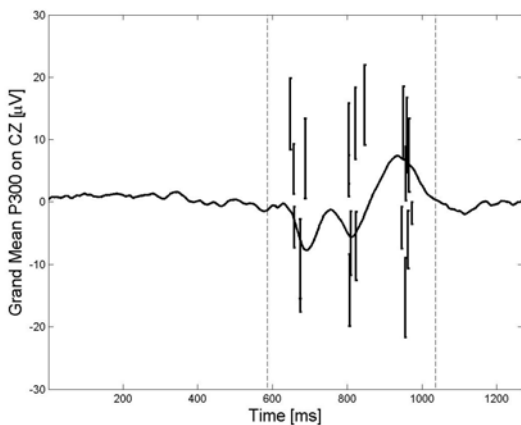


**Fig. 5** Mean amplitudes and standard deviation of various component groups plotted against the averaged P300 at Cz.

As mentioned in the data and method section, in order to illustrate the variability of the averaged P300, 10 random subsets, consisting of 40 trials selected out of 360 trials from 9 healthy participants, were formed and their averages at electrode Cz were calculated. Then, the P300 peaks were observed for these averaged subsets. The peaks, P1, N1, P2, and N2 were of different magnitudes in the different averages, and were sometimes absent, see Fig. (3). Furthermore, even the more prominent P3b peak looked reduced in amplitude as in plots 3 and 8 in Fig. (3). A similar procedure was repeated for each individual subject, with the same findings.

### 3.2 ICA procedure

Implementation of the ICA procedure resulted in 3475 independent components.

#### Artefact Removal, Feature Selection and Clustering

Using the artefact removal methods described above, 1485 artefacts were identified and removed. From the remaining 1990 components, the following features were extracted: the absolute values of the peaks of the back projected components within [586 1036] ms, the latencies of the peaks

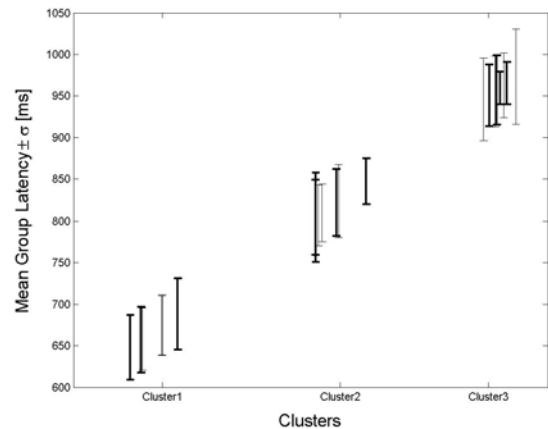


**Fig. 6** Mean latencies and standard deviation of various component groups. (Darker lines present the positively peaking components).

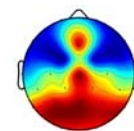
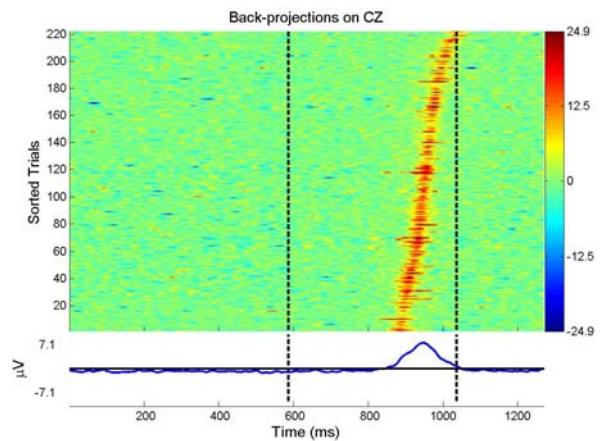


**Fig. 7** An ERP image of the P3b component type with its topography.

and the corresponding normalized columns of the mixing matrix.

The unsupervised k-means clustering algorithm described in the method section was applied and resulted in 3 main clusters containing 11 groups of components Fig. (4). Each of these 11 groups of components has similar latencies, absolute values of the peaks and topographies. The ratio of the positive components to the total number of components in each group varied from (0.0545) 5% (group 1-4) to (0.9407) 94% (group 3-4).

In Fig. 5 the mean amplitudes and standard deviation of various component groups are plotted against time together with the averaged P300 on Cz. Notice how these groups have latencies which overlap in Fig. 6, where the mean latencies

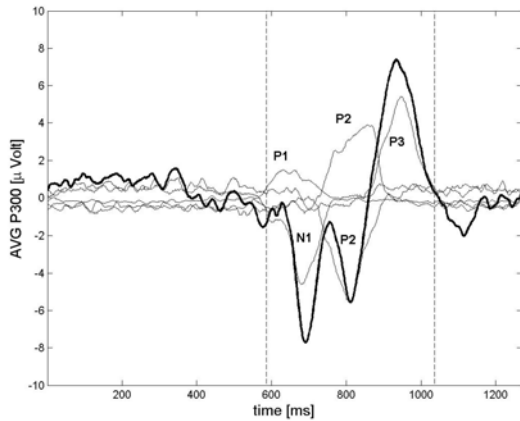


**Fig. 8** The averaged P300 on Cz (dark line) and the averages of the BICs constituting the P300.

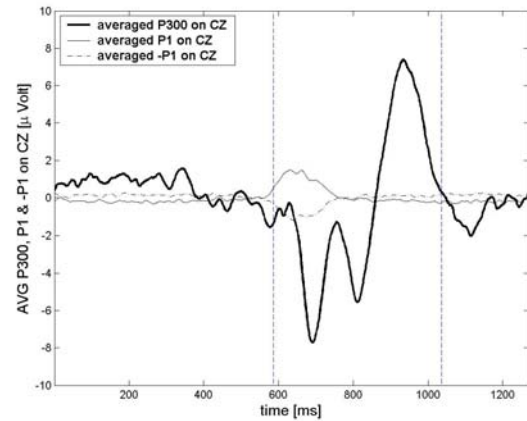


**Fig. 10** The averaged P300 on Cz (dark line), the averaged P1 and the corresponding averaged negative components (-P1) (dotted line).

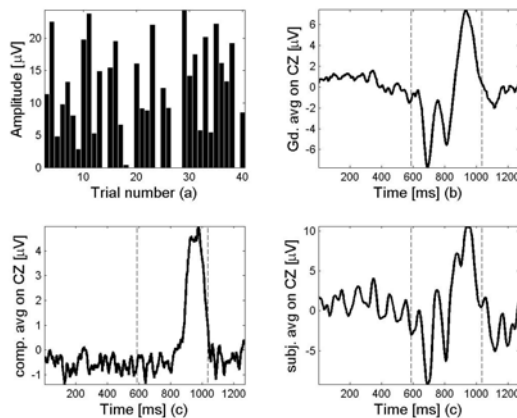


**Fig. 9** (a) A histogram of the P3b component for a randomly selected subject, (b) the grand average of the P300 on Cz, (c) the averaged P3b components belonging to the selected subject and (d) the averaged P300 on Cz for the selected subject.

and standard deviation of different component groups are plotted.

We were able to extract various component types which constitute the P300. For instance the P3b which is located in group 3-4 (222 ICs) is presented with its topography in Fig. 7. The mean latency of the P3b was found to be 365 [ms] (min = 300, max = 448 and SD = 37).

In addition to the 5 widely known components constituting the P300, a further 6 component types were extracted (not studied here). The averages of the 5 components constituting the P300 are plotted against the averaged P300 on Cz in Fig. 8.

### Trial-to-Trial Variation and the Peaks of the Averaged P300

It was observed that the resulting components did not appear in every single P300 trial. For instance, the P3b components

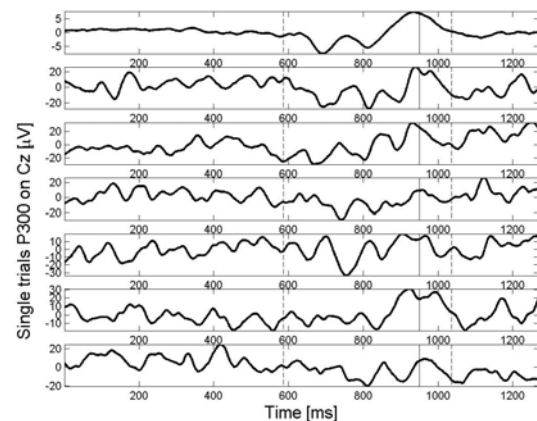


**Fig. 11** Single trial P300s corresponding to positive P3b. (Top plot is for the averaged P300 on Cz).

belonging to one subject (selected randomly) did not seem to appear in every trial (total of 40 trials). In Fig. 9 (a) the amplitudes of the P3b component for various trials were plotted against the trial number in which it appeared. The grand average of the P300 on Cz, the averaged P3b on Cz of the selected subject and the averaged P300 on Cz for the selected subject, respectively, are also shown. Not only did the P3b component not appear in every trial, but the magnitude of the P3b on Cz varied also, as can be seen.

Furthermore, not only were the P300 components missing in some trials, but also some components with reversed polarity appeared in different trials at nearly the same latency. For example, it is noticeable that P1 is reduced or nearly absent in the averaged P300, see Fig. 10. However, the average of the extracted positive P1 peak is apparent, and another less visible negative peak (-P1) occurs at nearly the same latency. This illustrates how the averaged P300 is dependent upon the positive and negative ICs; in this case nearly cancelling each other out in the averaged P300.

To make the above observation even clearer, a few of the P300 single trials on Cz corresponding to positive P3bs and



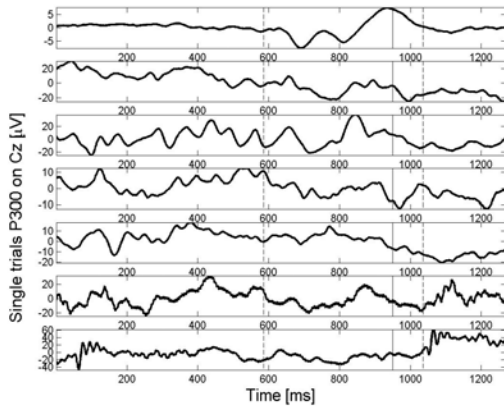


**Fig. 12** Single trial P300s corresponding to negative P3b. (Top plot is for the averaged P300 on Cz).

negative P3bs are illustrated in Fig. 11 and Fig. 12, respectively. The P3b appears consistently in the trials in Fig. 11 (top plot is for the averaged P300 on Cz), while the P3b is either missing or with negative polarity in Fig. 12.

Next, a few of single trial P300s corresponding to positive and negative P1 from only one subject selected randomly are illustrated in Fig. 13 and Fig. 14, respectively. The top plots in both figures present the averaged P300 on Cz for that particular subject.

#### 4 Discussion and conclusions

ICA was applied to single trial P300s, and a number of BICs were identified, which corresponded with known peaks in the P300 waveform, as well as some other components. The BICs were sparse, i.e. they were of short duration. Their shapes are described qualitatively as noisy half-sinusoids. The single trial P300 waveform is comprised of their sum.

It has been observed that there can be positive or negative BICs which occur at the same latency but over different trials. This was not only noted over trials recorded from various subjects, but also from recordings from the same subject. This trial-to-trial variation explains the variability in the averages of the P300 recordings as illustrated. This shows that the averaged P300 cannot be a sensitive biomarker, since it will depend upon the varying individual trial waveforms.

Since the BICs vary from trial-to-trial and some BICs will be missing in some trials, it may not be possible to derive biomarkers from single trial P300s in a straight forward manner. It will be necessary to characterise healthy subjects in terms of which BICs occur and how frequently, and to seek differences in the BICs of the P300 in other subject groups for which biomarkers are required, such as Alzheimer's patients. It is possible that certain BICs may be found to be more reliable biomarkers than the amplitude or latency of the commonly used P300b peak in the averaged P300. It is also important to explore the relationships among the BICs (inter-dependability) obtained from the same trial, which might be itself a biomarker which could distinguish other subject groups.

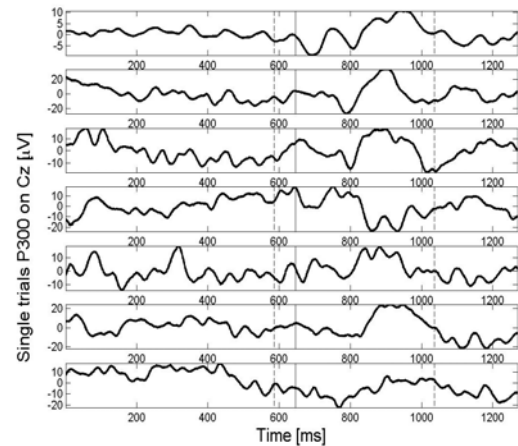


**Fig. 13** Single trial P300s corresponding to P1. (Top plot is for the averaged P300 on Cz).

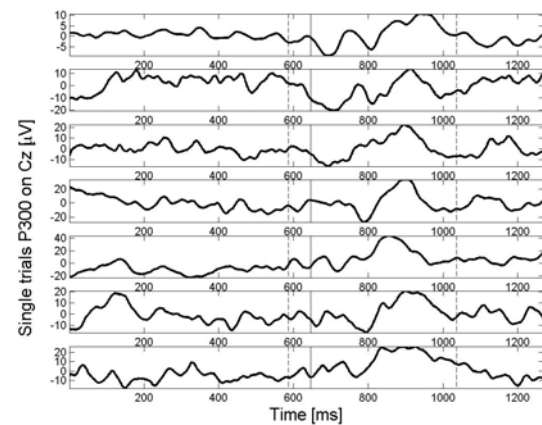


**Fig. 14** Single trial P300s corresponding to negative P1. (Top plot is for the averaged P300 on Cz).

#### Acknowledgements

This work was supported by Biopattern, IST EU funded project, Contract No. 508803.

#### References

- [1] A. J. Bell, T. J. Sejnowski, "An information-maximization approach to blind separation and blind deconvolution", *Neural Computations*, **volume 7**, pp. 1129-1159, (1995).
- [2] A. S. Gevins, "Analysis of the Electromagnetic Signals of the Human Brain: Milestones, Obstacles and Goals", *IEEE Trans Biomed Eng*, **volume 31**, pp. 833-850, (1984).
- [3] A. Tang, M. Shutterland and Y. Wang, "Contrasting single-trial ERPs between experimental manipulations: Improving differentiability by blind source separation", *NeuroImage*, **volume 29**, pp. 335-346, (2006).
- [4] C. Klein and B. Feige, "An independent components analysis (ICA) approach to the study of developmental differences in the saccadic contingent negative

- variation”, *Biological Psychology*, **volume 70**, pp. 105-114, (2005).
- [5] D. L. Davies, D. W. Bouldin, “A Cluster Separation Measure”, *IEEE Trans. on Pattern Anal. Mach. Intell.*, **volume 1**, pp. 224-227, (1979).
- [6] I. Jentzsch, “Independent Component Analysis separates sequence-sensitive ERP components”, *International Journal of Bifurcation*, **volume 14**, pp. 667-678. (2004).
- [7] J. B. MacQueen, “Some Methods for classification and Analysis of Multivariate Observations”, in *Proc 5<sup>th</sup> Berkeley Symposium on Mathematical Statistics and Probability*, Berkeley, California, USA, pp.281-297, (1967).
- [8] M. R. Nuwer, G. Comi, R. Emerson, A. Fuglsang-Frederiksen, J. M. Guerit, H. Hinrichs, A. Ikeda, F. J. C. Lucas and P. Rappelsburger, “IFCN standards for digital recording of clinical EEG”, *Electroencephalography and clinical Neurophysiology*, **volume 106**, pp. 259–261, (1998).
- [9] R. Johnson, “A triarchic model of P300 amplitude”, *Psychophysiology*, **volume 23**, pp.367-384, (1983).
- [10] S. A. Hillyard and M. Kutas, “Electrophysiology of cognitive processing”, *Ann. Rev. Psychol.*, **volume 34**, pp. 33-61, (1983).
- [11] S. Debener, S. Makeig, A. Delorme, A. K. Engel, “What is novel in the novelty oddball paradigm? Functional significance of the novelty P3 event-related potential as revealed by independent component analysis”, *Cognitive Brain Research*, **volume 22**, pp. 309-321, (2005).
- [12] S. Makeig, A. Delorme, M. Westerfield, T-P. Jung, J. Townsend, E. Courchesne, T. J. Sejnowski, “Electroencephalographic Brain Dynamics Following Manually Responded Visual Targets”, *PLOS Biology*, **volume 2**, pp. 747-762, (2004).
- [13] T-P. Jung, S. Makeig, M. Westerfield, J. Townsend, E. Courchesne and T. Sejnowski, “Analysis and visualisation of single-trial event-related potentials”, *Human Brain Mapping*, **volume 14**, pp.166-185, (2001).
- [14] T. W. Picton, D. T. Stuss, “The component structure of the human event-related potentials”, *Progress in Brain Research*, **volume 54**, pp.17-48, (1980).
- [15] W. Pritchard, M. Houlihan and J. Robinson, “P300 and response selection: A new look using independent-component analysis”, *Brain Topography*, **volume 12**, pp. 31-37, (1999).